Article

Effect of Land Use and Cover Change on Air Quality in Urban Sprawl

Bin Zou [1,2,*], Shan Xu [2], Troy Sternberg [3] and Xin Fang [2]

[1] Key Laboratory of Metallogenic Prediction of Nonferrous Metals and Geological Environment Monitoring, Ministry of Education, Changsha 410083, China

[2] School of Geosciences and Info-Physics, Central South University, Changsha 410083, China; 135011084@csu.edu.cn (S.X.); xinfang@csu.edu.cn (X.F.)

[3] School of Geography and Environment, University of Oxford, Oxford OX1 2JD, UK; troy.sternberg@geog.ox.ac.uk

[*] Correspondence: 210010@csu.edu.cn; Tel.: +86-731-88836502

Abstract: Due to the frequent urban air pollution episodes worldwide recently, decision-makers and government agencies are struggling for sustainable strategies to optimize urban land use/cover change (LUCC) and improve the air quality. This study, thus, aims to identify the underlying relationships between PM_{10} concentration variations and LUCC based on the simulated PM_{10} surfaces in 2006 and 2013 in the Changsha-Zhuzhou-Xiangtan agglomeration (CZT), using a regression modeling approach. LUCC variables and associated landscape indexes are developed and correlated with PM_{10} concentration variations at grid level. Results reveal that the overall mean PM_{10} concentrations in the CZT declined from 106.74 μg/m^3 to 94.37 μg/m^3 between 2006 and 2013. Generally, variations of PM_{10} concentrations are positively correlated with the increasing built-up area, and negatively correlated with the increase in forests. In newly-developed built-up areas, PM_{10} concentrations declined with the increment of the landscape shape index and the Shannon diversity index and increased with the growing Aggregation index and Contagion index. In other areas, however, the reverse happens. These results suggest that LUCC caused by urban sprawl might be an important factor for the PM_{10} concentration variation in the CZT. The influence of the landscape pattern on PM_{10} concentration may vary in different stages of urban development.

Keywords: urban sprawl; air quality; LUCC; landscape; urban agglomeration

1. Introduction

Urban sprawl, one of the most significant causes of the increasingly severe air pollution in the world [1–3], has made recent headlines in peer-reviewed journals of economics, urban planning, and public health [4–7]. As a direct result of urban sprawl, land use/cover changes (LUCC), as well as their spatial distribution (i.e., landscape pattern) variations may affect pollutants emission indirectly through industrial layout, travel behavior, and other human activities [3,8,9]. In view of the widespread health impacts of air pollution [10,11], studies have increasingly focused on the association between LUCC and air pollution variation caused by urban sprawl, including research on numerical simulations and empirical statistical modeling.

Numerical simulations refer to coupled modelling systems dealing with emissions from plants and traffic, and their dispersion-related meteorological and terrain factors. They are able to retrieve detailed air pollution distribution characteristics and address the complex links between LUCC, pollution discharge, weather patterns, and atmospheric chemistry. In this field, an early investigation was carried out by Civerolo, et al. [12]. They evaluated the influence of the increased urban land cover

and associated changes in ozone (O_3) concentrations in a future scenario, and concluded that land cover changes may lead to O_3 variation. A study conducted by De Ridder, et al. disclosed that urban sprawl in the German Ruhr area could generate higher O_3 and PM_{10} concentrations [13]. More recently, Kahyaoğlu-Koračin, et al. evaluated a set of alternative future patterns of land use and found out a Regional Low-Density Future has the greatest impact on air quality [14]. Martins, using a sequential modeling process, also concluded that urban sprawl increases PM_{10} annual average values [5]. However, their reliance on abundant data (e.g., emission inventories, meteorological data, land-surface scheme) for numerical diffusion makes interpretation difficult [15] and incurs high computational costs.

Empirical statistical models provide a relatively simple and direct method to demonstrate the importance of land use to air quality at various scales. Weng and Yang investigated the relationship of local air pollution patterns to urban land use through Geographic Information System (GIS) and correlation analysis [16]. They found that the spatial patterns of air pollutants are positively correlated with the built-up density. Bereitschaft and Debbage employed stepwise linear regression to quantify the relationship between air pollution and urban form variables (e.g., land use diversity) in 86 U.S. metropolitan areas, and their findings are consistent with that of prior modeling researches [17]. Another example is given by Weber, et al. who concluded that landscape metrics are very useful in predicting PM_{10} exposure [18]. Using urban landscape metrics framework, McCarty and Kaza found the mix of different land cover types identifies important correlations between pollutant levels and air quality [19]. Unfortunately, their effectiveness is limited since the formation mechanisms of air pollution are generally overlooked in these studies. Additionally, these studies usually take the group mean of concentrations at monitoring sites across a city as statistical samples and this could lead to the interpretive problems due to the ignorance of spatial heterogeneity between changes in air pollution and LUCC inside the city.

Land use regression (LUR) models can effectively estimate the spatially-resolved air pollution under conditions of sparse measurements [15,20–23]. In this process, the LUR uses monitored pollutant concentrations as the dependent variable, and takes surrounding land use, transportation and other variables obtained through GIS as predictors [24,25]. It offers a rough, yet helpful, perspective on the analysis of the relationship between the urban LUCC and air pollution variation and attaches certain positive significance to the rational evaluation of city planning and land use strategies. However, as the land-use are generally not time varying and their temporal resolution tends to be limited, few studies have paid attention to the transferability of the LUR model across time [26,27]. Meanwhile, although the LUR has been promoted in many developed countries, relatively few studies have been conducted in China. More importantly, as one of the heaviest air pollution countries in the world [28–30], China's urbanization rate increased from 17.92% in 1978 to 53.73% in 2013. This process results in a large loss of natural land and a rather chaotic landscape pattern [7]. Therefore, characterizing the spatial patterns of air pollutants in China can bring us more complete understanding of the comprehensive effect of LUCC on air quality worldwide.

Especially, a policy to develop a resource-conserving and environmentally-friendly society (i.e., the "Two Oriented Society" policy) had been started in China since 2006. As one of the first two areas in China that performed the policy, the Changsha-Zhuzhou-Xiangtan agglomeration (CZT) attempted to direct viable use of resources, conservative consumption of energy, ecological protection, as well as pollution prevention and treatment. Hence, taking the CZT as a case to evaluate the air quality variations before and after the "Two Oriented Society" strategy implementation can be a touchstone of the policy and could provide an unprecedented chance to deeply understand whether urban planning and land use policies may improve air quality.

This study employed remote sensing technologies and the LUR model to acquire the LUCC and simulated PM_{10} concentration surfaces in the CZT for years 2006 and 2013. Based on the hypothesis that the LUR model possesses transferability over time in the CZT area, we attempted to address the following questions: (1) Is the government strategy for sustainable construction and development an effective policy to improve air quality in urban areas? (2) Does the LUCC in the study area correlate with the estimated variation in air pollution, and (3) if so, what is the current trend?

2. Materials and Methods

2.1. Study Domain

The Changsha-Zhuzhou-Xiangtan agglomeration (CZT) is located in the northeast of Hunan province in China, comprising the cities of Changsha, Zhuzhou and Xiangtan (Figure 1). The CZT covers an area of 28,087 km^2, and has a population of 13.78 million. In terms of transportation, the CZT is a national traffic hub, linked together by a comprehensive railway system, as well as major arterial road networks. The Xiangjiang River flows through this area in a way that promotes efficient goods movement. The CZT is the most important industrial base and the economic growth hub of Hunan Province with an urbanization rate of 61.0% in 2013, 17.7% higher than the rest of Hunan and 7.3% greater than the national average. However, with these achievements, these three cities are the major pollution emission sources in Hunan province.
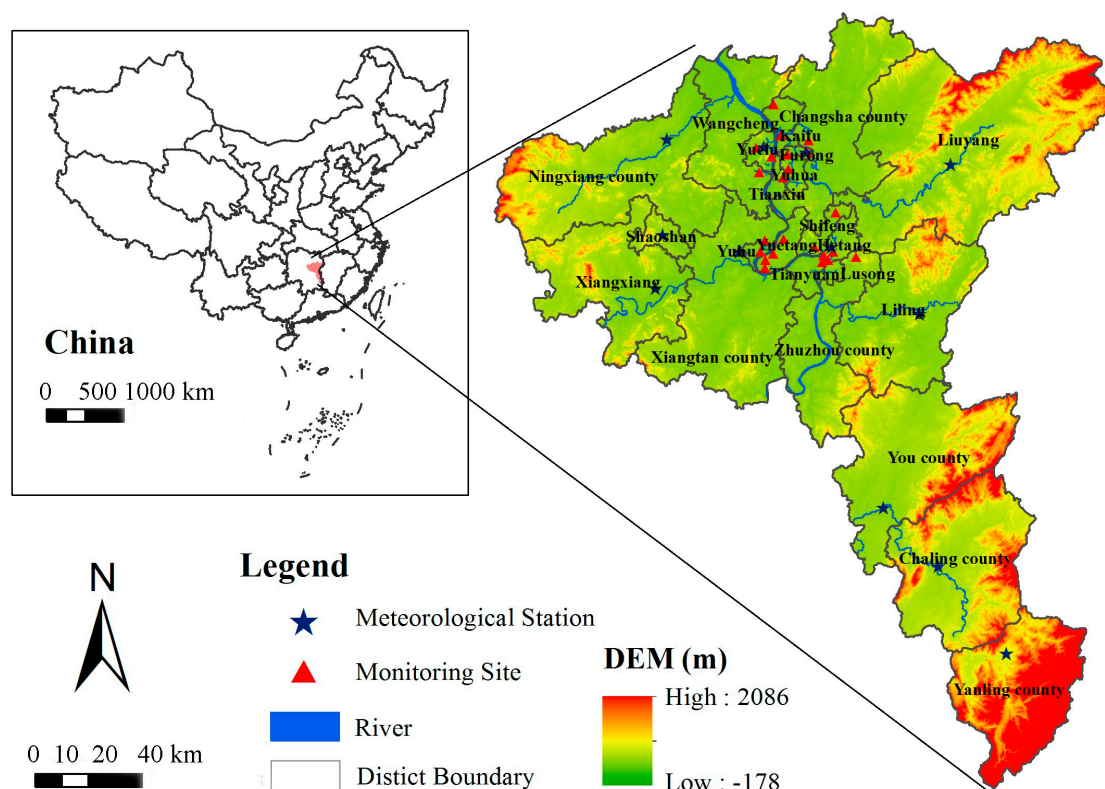
Figure 1. Study domain, the Chang-Zhu-Tan agglomeration.

2.2. LUCC Monitoring

2.2.1. Land Use/Cover Classification

Materials used for monitoring land use include cloud-free Landsat TM (for 2006) and Landsat OLI images (for 2013) in the same time phase. Data were downloaded from the United States Geological Survey (USGS) database [31]. Taking the land cover features of the CZT into account, a modified version of the land use classification was developed [3,16]. The categories include: (1) water, (2) bare soil, (3) built-up, (4) agricultural land, (5) forest, and (6) green land. Green land refers to the open forest land, grass land, and urban green land (i.e., parks, lawns, and other urban open green spaces). They tend to have a disconnected and scattered distribution and share similar spectra characteristics in the study area, which means it is difficult to separate them from each other. And the land use classification was implemented by the maximum likelihood algorithm in ENVI 5.2 [32]. The results are raster maps with a resolution of 30 m. These grid maps of area proportion of each land use were then reclassified

into 1 km $\times$ 1 km resolution to compare with the spatial patterns of PM$_{10}$ concentrations simulated by the LUR model.

2.2.2. Landscape Pattern

Landscape metrics are algorithms that quantify a specific spatial configuration of various land use/covers [33,34]. Considering the diversity and heterogeneity of landscape [35,36], five representative landscape-level metrics characterizing the urban sprawl were calculated by Fragstats 4.0 based on the resampled land use maps with a resolution of 1 km $\times$ 1 km [37]. The metrics include Aggregation index (AI), Contagion index (CONTAG), Landscape shape index (LSI), Perimeter-area fractal dimension (PAFRAC), and Shannon's diversity index (SHDI). They can be expressed by Equations (1) to (5):

$$\text{AI} = \left[\Sigma_{i=1}^{m}\left(g_{ii}/\max - g_{ii}\right)P_i\right](100) \tag{1}$$

$$\text{CONTAG} = \left\{1 + \left[2\ln(m)\right]^{-1}\Sigma_{i=1}^{m}\Sigma_{k=1}^{m}\left[(P_i)\left(g_{ik}/\Sigma_{k=1}^{m}g_{ik}\right)\right]\left[\ln(P_i)\left(g_{ik}/\Sigma_{k=1}^{m}g_{ik}\right)\right]\right\}(100) \tag{2}$$

$$\text{LSI} = 0.25\,E^{*}/\sqrt{A} \tag{3}$$

$$\text{PAFRAC} = 2\{[N\Sigma_{i=1}^{m}\Sigma_{j=1}^{n}\left(\ln p_{ij}a_{ij}\right)] - [(\Sigma_{i=1}^{m}\Sigma_{j=1}^{n}\ln p_{ij})(\Sigma_{i=1}^{m}\Sigma_{j=1}^{n}\ln a_{ij})]\}^{-1}/[(N\Sigma_{i=1}^{m}\Sigma_{j=1}^{n}\ln p_{ij}^2)(\Sigma_{i=1}^{m}\Sigma_{j=1}^{n}\ln p_{ij})^2] \tag{4}$$

$$\text{SHDI} = -\Sigma_{i=1}^{m}\left(P_i \ln P_i\right) \tag{5}$$

where g_{ii} and g_{ik} are the number of like adjacencies (joins) between pixels of patch type (class) i obtained by the single-count and double-count method, respectively, and max-g_{ii} is the maximum g_{ii}. P_i is the proportion of patch type (class) i. m and n are the number of patch types and classes present in the landscape. E^{*} refers to the total edge length (*meter*) of the landscape, while A is the total area (m^2). a_{ij} and p_{ij} are area (m^2) and perimeter (*meter*) of patch ij. N is the total number of patches in the landscape.

Among the above five landscape-level metrics, AI is an index measuring the amount of the maximum possible number of like adjacencies given any landscape composition. Higher AI values indicate more aggregative patches of the same type. A landscape with interspersed patch types will have relatively low CONTAG values. While a single patch type occupies a very large percentage of the landscape, the CONTAG is high. The greater the value of LSI, the more dispersed the patch types. If patches have simple geometric shapes, the PAFRAC will be relatively low. The greater the value of SHDI, the richer the land use types.

2.3. PM$_{10}$ Concentration Estimation

2.3.1. Monitoring Data

Daily PM$_{10}$ mass concentrations in 2013 were collected from the official website of the China Environmental Monitoring Center [38]. Annual mean values of these observations were calculated for model fitting afterward. There are 23 monitoring sites constantly operated by local government agencies since 1 January 2013. Among them, 10 are in Changsha, seven in Zhuzhou, and six in Xiangtan. In addition, we obtained the annual average PM$_{10}$ concentrations at sven monitoring sites in Changsha of 2006 to validate the transferability of the lateral LUR model of 2013 (referred to as LUR model 2013 hereafter) over time in this study.

2.3.2. Predictor Variables

Similar to previous reported LUR modeling researches [24], correlation analysis is needed to identify possible predictors. The predictor variables identified in this study include area proportions of each land use, road length, and the distance to a nearest major road, as well as the population density. They are generated at buffers with different radius (50–5000 m) of each monitoring site, so the selection of buffer size plays an important role in determining the performance of the LUR model [24]. Moreover, the annual averages of Aerosol Optical Depth (AOD) measurements of the 23 monitoring sites were

extracted from the MODIS Terra data (MOD04 Level 2 Collection 5, at a 10×10 km spatial resolution) obtained by the US-based National Aeronautics and Space Administration (NASA) [39]. Other potential variables include elevation, urban fractal dimension, contagion, and surface meteorological elements (i.e., relative humidity, temperature, precipitation, and wind speed). Population and elevation statistical data were made available by the Statistical Bureau of Hunan Province and USGS [40], respectively. Meteorological data were released by the Hunan Meteorology Bureau [41]. All variables (Table 1) were extracted by ArcGIS10.0.

Table 1. Potential predictor variables.

GIS Dataset	Predictor Variables	Unit	Buffer Size (Radius in Meters)
Land use variables	Water	%	
	Bare soil	%	
	Built-up area	%	100, 200, 300, 400, 500, 600, 700, 800,
	Agricultural land	%	900, 1000, 2000, 3000, 4000, 5000
	Forest	%	
	Green land	%	
Traffic variables	Major road length	Kilometer	50, 100, 200, 300, 400, 500, 600, 700, 800, 900, 1000, 2000, 3000, 4000, 5000
	Distance to a nearest major road	Kilometer	NA
Population	Population density	Thousand persons per square kilometer	NA
Meteorological parameters	Relative humidity	%	NA
	Temperature	Celsius degree	NA
	Precipitation	Millimeter	NA
	Wind speed	Meter/s	NA
Other urban characteristics	Elevation	Meter	NA
	Fractal dimension	NA	NA
	Contagion	NA	NA
MODIS	Aerosol Optical Depth	NA	NA

2.3.3. Land Use Regression Modeling and Validation

A general LUR model can be defined as follows:

$$PM_{10,s} = a_0 + a_1 X_{1,s} + a_2 X_{2,s} + \ldots + a_n X_{n,s} + \mu \tag{6}$$

where $PM_{10,s}$ is the estimation of the annual average PM_{10} concentration, and is regarded as the dependent variables of site s, $X_{i,s}$ ($i = 1, 2, \ldots n$) are independent variables, a_k ($k = 0, 1, 2, 3$) are the regression coefficients estimated, and μ is the random error under the condition that the value of $\Sigma_{i=1}^{s}(PM_{10,1} - P\hat{M}_{10, i})$ is minimized over the observations.

In this study, LUR models were conducted using a supervised stepwise regression. In this process, we first separately entered each potential predictor derived from 2013 to identify which one could explain the largest variance. Second, we evaluated whether other added variables will lead to an increase larger than 1% in the adjusted R^2. This procedure was repeated until no more variables entered the model. We also calculated the collinearity statistics, such as the tolerance and variance inflation factor (VIF). It should be noted that variables can only be entered in the model when the coefficients are statistically significant and there is no multicollinearity between these variables. Additionally, statistics including the model fitting R^2, root mean square error (*RMSE*), standard deviation (*SD*), mean relative tolerance (*MRT*), as well as the CV R^2 were employed to evaluate the prediction ability and reliability of the LUR model of year 2013 based on the Leave-One-Out-Cross-Validation (LOOCV) method.

For visualization purposes, we created nearly 27,900 lattice points with a resolution of 1 km $\times$ 1 km, where PM_{10} concentrations were then predicted using the LUR model of year 2013

based on PM_{10} concentrations at those lattice points. Finally, a smooth surface was interpolated through the inverse distance weighting (IDW) method. It has to be noted that the PM_{10} concentrations of year 2006 was also estimated by the LUR model of year 2013 in order to test the transferability of LUR models over time in this study.

2.4. LUCC and PM_{10} Variations

To test the assumed link between LUCC and PM_{10} variation during the urban sprawl process, we first obtained the area proportion of each LUCC and associated landscape metrics at a resolution of 1 km×1 km for years 2006 and 2013. Second, raster calculators were used to extract variations of PM_{10} concentrations and area proportion of each LUCC, as well as that of landscape metrics, which were then employed for quantitative comparison and correlation analyses. Pearson's correlations with *P* values were calculated using SPSS software (version 19.0) [42].

3. Results

3.1. Land Use/Cover and Landscape Pattern in 2006 and 2013

Results of the land use/cover classification are presented in Figure 2a. The overall classification accuracy is 83.57% for the 2013 map and 80.04% for the 2006 map. As we can see, built-up areas are distributed mainly along the Xiangjiang River. From 2006–2013, their proportion increased by 4.79%, from 2984 km^2 to 3134 km^2. These increased built-up lands are mostly converted from agricultural land and forest, whose area decreased 15 km^2 and 98 km^2, respectively. The bare soil increased from 4.16% to 6.49% and green land decreased from 9.27% to 6.85%. The change of water area (from 556 km^2 to 543 km^2) is small.

Figure 2b–f illustrate that the spatial distribution of landscape metrics in the CZT of years 2006 and 2013 are similar. The southern and eastern CZT have high AI (>63) and CONTAG (>52), but low LSI (<2.1), PAFRAC (<1.40), and SHDI (<0.91). AI closely resembles CONTAG in spatial patterns, which is contradictory to that of LSI and SHDI. Inner urban areas of the CZT (i.e., Kaifu, Yuelu, Furong, Yuhua, Tianxin, Yuhu, Yuetang, Hetang, Shifeng and Lusong districts) have rather high AI, CONTAG, and low LSI, PAFRAC, SHDI in 2013, greater than those in 2006.
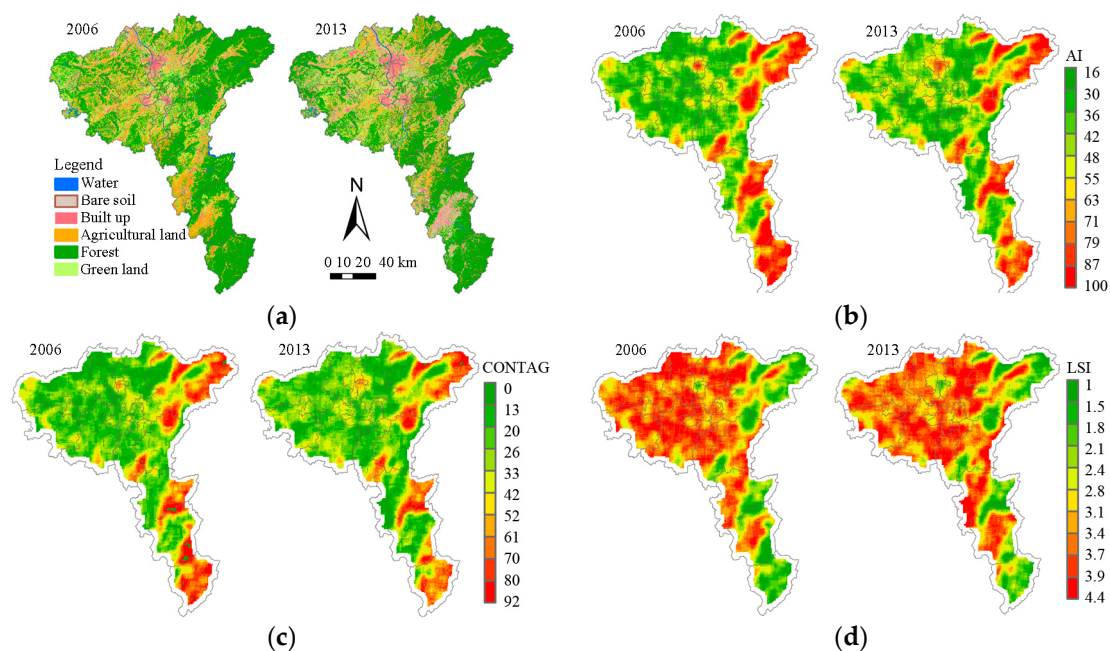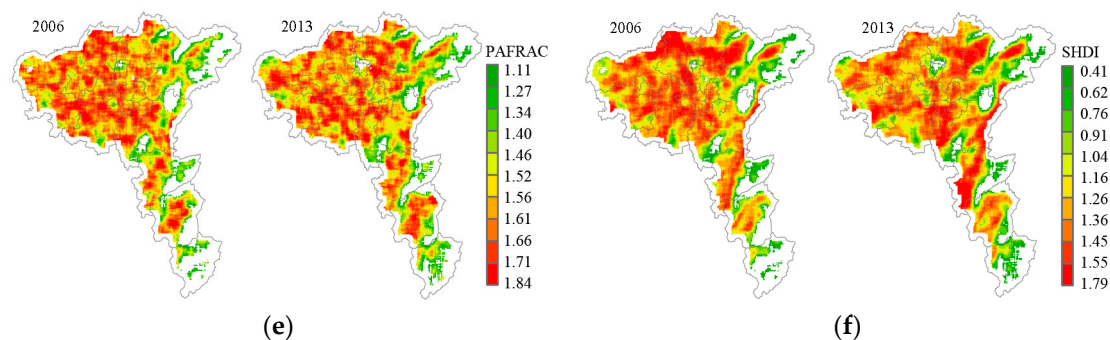

Figure 2. *Cont.*

Figure 2. (**a**) Land use/cover; (**b**) spatial patterns of Aggregation index (AI); (**c**) spatial patterns of Contagion index (CONTAG); (**d**) spatial patterns of Landscape shape index (LSI); (**e**) spatial patterns of Perimeter-area fractal dimension (PAFRAC); and (**f**) spatial patterns of Shannon's diversity index (SHDI), in the CZT.

3.2. LUR Model Development and Validation

As is shown in Table 2, the proportions of built up area, bare soil, road length, and relative humidity are highly significant predictors ($p < 0.05$) of PM_{10} concentrations in the CZT. While the built up area proportion in the monitoring site buffer zone (with a width of 900 m) shows positive estimated power (58.37 ± 12.55), it does for the bare soil area proportion within the 300 m buffer (11.64 ± 3.05). Relative to the negatively-estimated power of the major road length within the 300 m buffer around monitoring sites (−9.76 ± 3.19), the increased relative humidity (4.25 ± 1.86) would correspond to higher PM_{10} concentrations. Additionally, the VIF (<2) shows no multiple correlations among the independent variables.

Table 2. Estimated regression coefficients of the final model.

| Model Variable	Unstandardized Coefficients		*t*	Sig.	Collinearity Statistics	
	B	Std. Error			Tolerance	VIF
(Constant)	125.80	3.24	38.84	<0.0001	0.937	1.068
Built up_900m	58.37	12.55	4.65	<0.0001	0.581	1.722
Bare soil_300m	11.64	3.05	3.81	0.001	0.573	1.746
Road length_300m	−9.76	3.19	−3.06	0.007	0.896	1.116
Relative humidity	4.25	1.86	2.29	0.035	0.937	1.068

Table 3 summarizes model fitting and validation results for the LUR model of year 2013 and its transferability application evaluation in year 2006. It can be seen that the linearity between PM_{10} concentrations and its explanatory variables are significant (Sig. *F* < 0.0001). The final model has a RMSE of 9.36 μg/m^3. Meanwhile, the adjusted overall mean R^2 is 0.62, meaning the model can explain 62% of the PM_{10} concentration variations. Comparatively, the mean R^2 of LOOCV is 0.69, and it ranges from 0.63 to 0.75 for each site, while the CV R^2 is also acceptable with a value of 0.56. Model-based SD and CV RMSE are 11.09 μg/m^3 and 10.86 μg/m^3, respectively. The MRT for validation is 8.10% with the relative error of predictions varying from 0.04% to 22.81%. In addition, validation results based on seven monitoring sites in 2006 in Table 3 also confirm the transferability of the LUR model 2013 with the MRT at 7.24% and RMSE at 7.24 μg/m^3.

Table 3. Model performance and validation of LUR model developed in this study.

Model Performance		Leave-One-out Cross Validation		Validation of 2006	
R^2	0.69	R^2	0.69		
Adjusted R^2	0.62	CV R^2	0.56		
RMSE	9.36	MRT	8.10	MRT	7.24
Sig. *F*	<0.0001	CV RMSE	10.86	RMSE	9.87
		SD	11.09		

3.3. Spatial Distribution Mapping of PM$_{10}$ Concentrations in 2006 and 2013

Figure 3 shows the distribution of the estimated PM$_{10}$ concentrations of years 2006 and 2013 over the entire CZT. Generally, spatial variability can be found with average PM$_{10}$ concentrations from 54 to 148 μg/m^3. As expected, dense urban areas in the CZT have higher PM$_{10}$ concentrations, while suburban and rural areas usually relate to low PM$_{10}$ concentrations. The three most polluted districts in 2006 are Furong, Yuhu, and Yuhua, with mean PM$_{10}$ concentrations 122.80 μg/m^3, 123.93 μg/m^3, and 125.27 μg/m^3, respectively. In 2013, the most polluted districts are Yuhua district (116.80 μg/m^3), Yuetang district (119.64 μg/m^3), and Yuhu district (132.23 μg/m^3). From 2006–2013, the overall mean PM$_{10}$ concentrations decreased from 106.74 μg/m^3 to 94.37μg/m^3, even though some areas of north Yuelu district (from 109.02 μg/m^3 to 114.15 μg/m^3), east Zhuzhou city (from 108.33 μg/m^3 to 115.95 μg/m^3), and Lusong district (from 100.04 μg/m^3 to 114.81 μg/m^3) show signs of deterioration in air quality. In this process, nine of the twelve districts in the central CZT show slight increment (around 5 μg/m^3) in mean PM$_{10}$ concentrations (i.e., Kaifu, Yuelu, Yuhu, Lusong, Shifeng, Hetang districts), while, the most southern and western Xiangtan County have witnessed an outstanding decline (from 114.42 μg/m^3 to 101.97 μg/m^3) of PM$_{10}$ concentrations during this period.
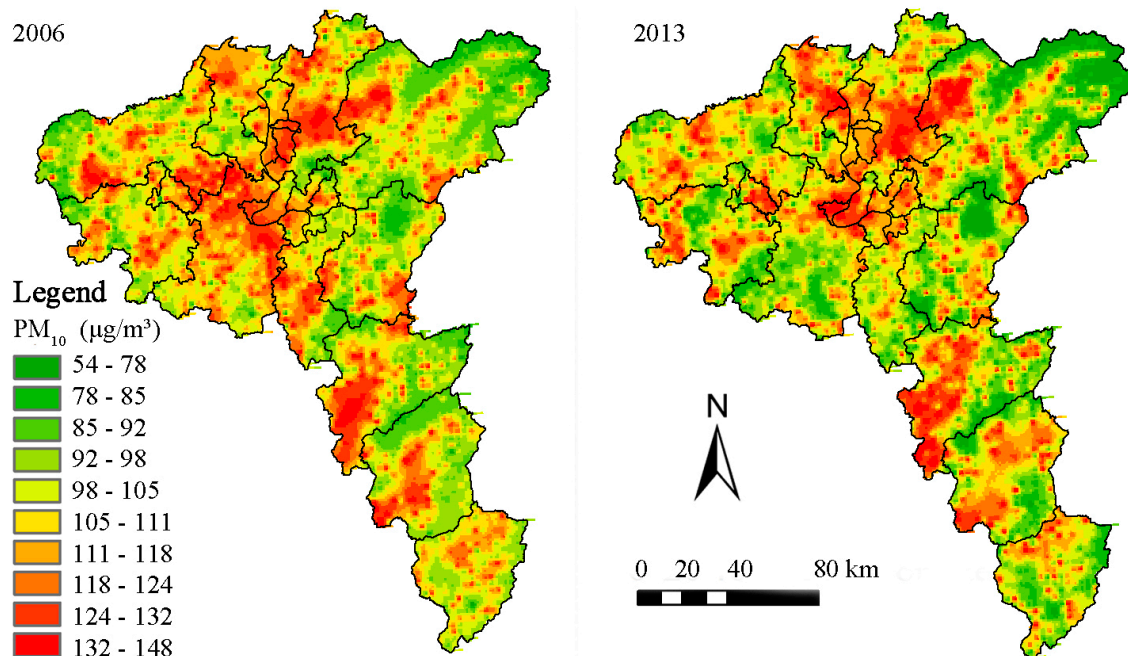

Figure 3. Spatial distributions of PM$_{10}$ concentration in 2006 and 2013.

3.4. Impacts of LUCC on PM$_{10}$ Concentration Variation

Figure 4 shows the change in PM$_{10}$ concentrations and area proportions of each land use from 2006 to 2013. In general, most PM$_{10}$ concentration increase occurs around the inner CZT, where the forest disappeared drastically and construction expanded rapidly (e.g., the southern Changsha County, and

northern Yuelu and Wangcheng districts). PM_{10} concentration increased strikingly with the growing area proportion of bare soil in the southern Changsha County and southwestern Shaoshan County. The northeastern Chaling County experienced a complex change in land use. For most grids, more than 25% of land has changed its original use. These places show a clear increase in PM_{10} concentrations.
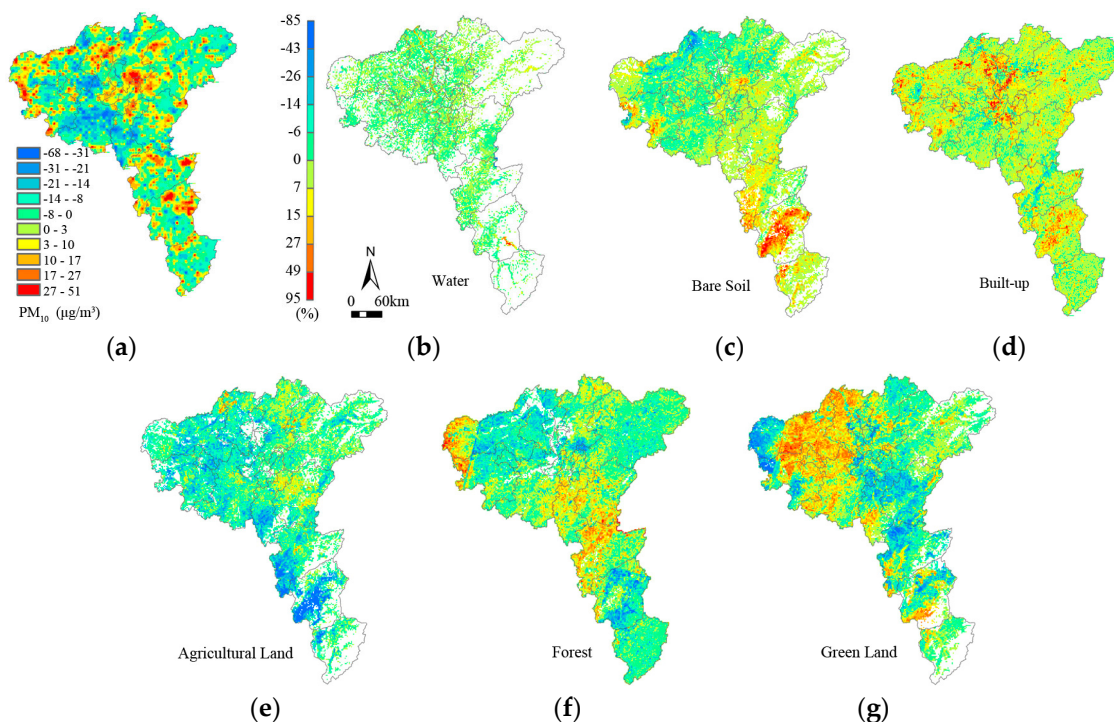
Figure 4. (**a**) Variations of PM_{10} concentrations and variations of area proportions of (**b**) water; (**c**) bare soil; (**d**) built-up areas; (**e**) agricultural land; (**f**) forest; and (**g**) green land.

Moreover, results from correlation analysis (Table 4) further confirm effect of LUCC on air pollution. PM_{10} concentration variation has a positive relation with the proportion changes of built-up area, bare soil, and agricultural land, and is negatively correlated with that of forest and green land ($p < 0.0001$). The sensitivity sequence of these five types of land use from high to low is built-up > green land > bare soil > forest > agricultural land. Meanwhile, the proportion change of water area is found to be the weakest predictor of PM_{10} concentration variation ($r = -0.023$; $p = 0.297$).

Table 4. Pearson correlation coefficients between PM_{10} concentration variation and area proportion change of each land use.

Land Use Types	Water	Bare Soil	Built up	Agricultural Land	Forest	Green Land
Correlation coefficient	−0.023	0.178	0.221	0.073	−0.153	−0.180
Sig. (2-tailed)	0.297	<0.0001	<0.0001	<0.0001	<0.0001	<0.0001

3.5. Impacts of Landscape Change on PM_{10} Concentration Variation

Clearly, the increased LSI, PAFRAC, and SHDI and the decreased AI, and CONTAG relate to PM_{10} concentration increase in the east and south suburban and rural areas of the CZT (Figure 5). In the newly-developed built-up area of the inner urban areas (i.e., the northern Yuelu district and the area adjacent to Wangcheng district, Yuetang district, and Xiangtan County), PM_{10} concentration increases with the growing AI and CONTAG and decreases with the increment of LSI and SHDI. Conversely, PM_{10} concentration shows a decline in eastern Ningxiang County and mid-western Xiangtan County where the AI and CONTAG increased greatly, but LSI and SHDI decreased.
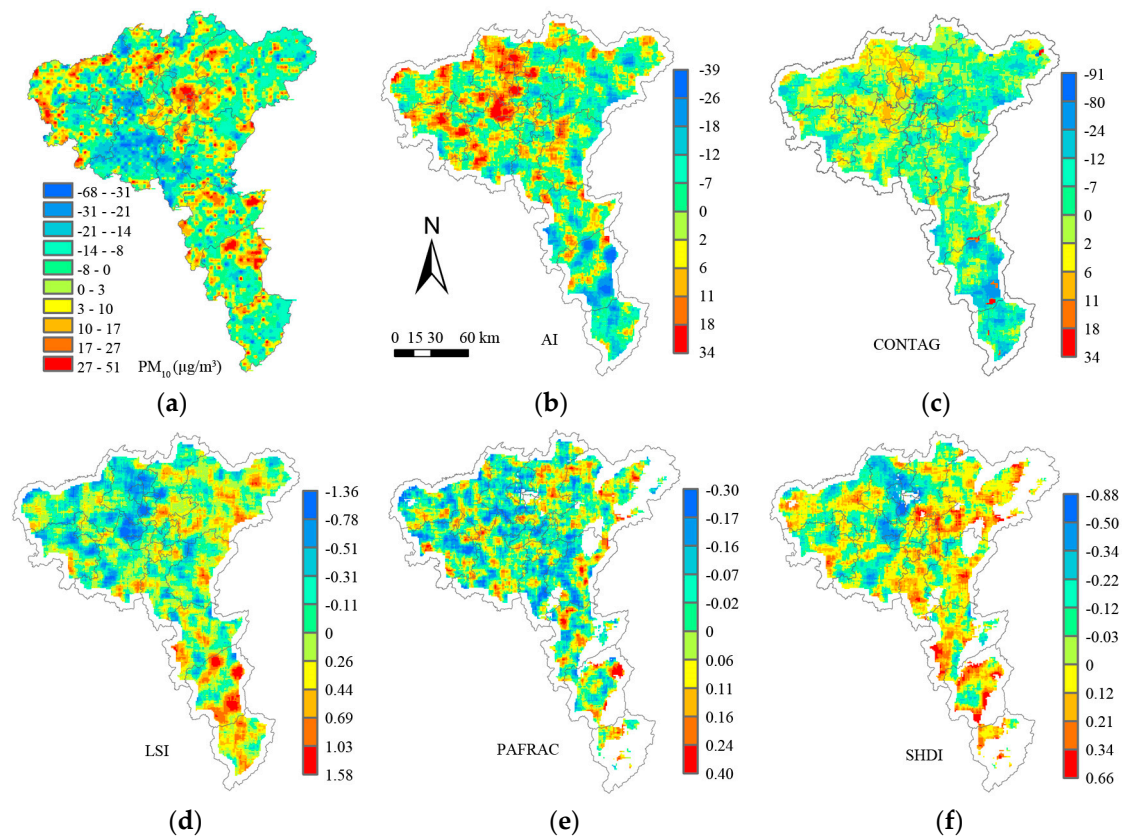
Figure 5. (**a**) Variation of PM_{10} concentration and Variation of (**b**) AI; (**c**) CONTAG; (**d**) LSI; (**e**) PAFRAC; (**f**) SHDI.

Table 5 further demonstrates the correlations between the variations of landscape metrics and PM_{10} concentration changes. On one hand, changes of AI ($r = -0.097$) and CONTAG ($r = -0.114$) negatively correlate with the changes of PM_{10} concentrations ($p < 0.0001$). On the other hand, positive correlations between the changes of landscape metrics and PM_{10} concentrations follows a typical declined sequence of SHDI ($r = 0.060$, $p = 0.004$) and LSI ($r = 0.046$, $p = 0.024$). However, no statistically significant correlation between changes of PAFRAC and PM_{10} concentration ($p = 0.866$) was found.

Table 5. Pearson correlation coefficients between changes of PM_{10} concentrations and landscape metrics.

Land Use Types	AI	CONTAG	LSI	PAFRAC	SHDI
Correlation coefficient	−0.097	−0.114	0.046	0.004	0.060
Sig. (2-tailed)	<0.0001	<0.0001	0.024	0.866	0.004

4. Discussion

Fine-resolution monitoring data for air pollutants are rarely available for most countries in the world [22]. Prefecture-level cities in China, for example, had no continuous automatic air pollution monitoring system until 2013. In order to estimate air pollution in suburban and rural areas distant from monitoring sites in the CZT urban agglomeration, a LUR model, called LUR model of year 2013, was developed and its transferability across time was also validated in this study. The LOOCV R^2 (0.63–0.75) and absolute bias (MRT 0.04%–22.81%) of this developed LUR model demonstrate comparable reliability to previously-reported LUR models with R^2 ranging from 0.22 to 0.72 and absolute bias ranging from 17% to 22% [21,23].

Based on the data of consumption proportions of raw coal, petroleum, natural gas, clean energy (i.e., hydropower, nuclear power, wind power, etc.) and other sources in 2006 (68.51%, 12.87%, 0.66%, 14.87%, 3.09%, respectively) and 2013 (62.23%, 11.66%, 1.55%, 14.04%, 10.52%, respectively) of the CZT are [43] and given the efficient and conservative use of energy has been promoted by the 'Two Oriented Society' policy, we assume the change of energy production and consumption structure in the study region has been stable. This could be the reason why the estimated PM_{10} concentrations in 2006 can be accurately predicted by the LUR model 2013 in this study, and also indicates the potential transferability of the LUR model 2013 across time in the CZT area.

Temporal variation in PM_{10} concentrations suggests that the "Two Oriented Society" policy has positive effect on reducing PM_{10} concentration. The overall mean PM_{10} concentration in the CZT has decreased since it became a national comprehensive supporting trial area in the implementation of this policies. In this process, the local governments encourage building greening systems along the urban streets, afforesting waste hills or unclaimed lands, and converting low farmlands into lakes. Moreover, high-tech industrial and science parks are gradually replacing original disordered productive land use (i.e., industrial, warehouse, mining). These actions not only cut down the emissions of possible LUCC related pollution sources, but also blocked the pollutants dispersion. However, as a consequence of the three cities (Changsha, Zhuzhou, and Xiangtan City) joining together and the accelerated industrial development, air pollution in the central CZT is still very challenging. Efforts for emission reduction and air pollution prevention and treatment should especially be put on the inner urban agglomeration, and these actions could be implemented by the incorporations in land use, economic development, industrial layout, and traffic pattern among three cities.

The association between LUCC and PM_{10} concentration variation clearly illustrates the potential contribution of land planning in reducing air pollution. The change of forest area shows a negative influence on PM_{10} concentration that is strongly positively correlated with the increasing built-up area. This result confirms findings of Weng et al. and Stone [4,16], suggesting that land use strategies including creating urban growth boundaries (i.e., restricting peripheral spread of urban zones and the resulting vehicle increase) and protecting essential ecological sites would be effective in limiting PM_{10} concentration growth [13]. Reduction of green space relates to PM_{10} increase, corroborating its important role in mitigating air pollution. The positive relationship between PM_{10} variation and bare soil proportion change may be induced by the ground dust. The tidal wave of migrant workers leaves a broad agricultural land out of cultivation, which may increase the PM_{10} concentration. Additionally, straw burning is one of the major sources of PM_{10} in the autumn.

For landscape, the changes of LSI, SHDI, and PAFRAC have positive correlation with the PM_{10} concentration variation in suburban and rural areas. The increase of these landscape metrics could be significant signals of human disturbance to predominant, continuous patches of natural landscape [18]. Growing human activities are bound to increase energy and transport demands, which have positive effect on PM_{10} concentration. On the other hand, the dominant landscapes in these areas covering over two-thirds of the study area are forest and green land, with high AI and CONTAG, and little pollutant source, hence the PM_{10} concentration is rather low. This reconfirmed the results of Liu and Shen [44]. However, the newly developed built-up area is experiencing a decrease of LSI and SHDI whilst an increase of AI, CONTAG, and PM_{10} concentration. A possible reason of this could be the concentration of buildings in a small area with simple geometric shapes and high traffic emissions. Moreover, the resultant air pollutant may be entrained in a re-circulatory system due to the "street canyons effect" [45]. All of these indicate that the landscape impact on PM_{10} concentration in the study area is closely related to the development stage it is in.

5. Conclusions

This study developed a LUR model that coupled land use and meteorology factors to evaluate the effect of urban LUCC on air pollution variation during the urban sprawl of the CZT from 2006–2013. While the proposed LUR model of year 2013 was validated in terms of transferability in the CZT

with relatively stable energy production and consumption structure across time, this study disclosed that the PM_{10} concentrations in the CZT have generally decreased after the implementation of the "Two-Orientated society" policy since 2006. The urban LUCC, including land cover and landscape, influences PM_{10} variations. Increases of built-up areas and decreases of forest areas during the period from 2006–2013 have considerable adverse impacts on PM_{10} variation, while the effects of landscape pattern variation are only moderate, and these effects vary in newly-developed built-up areas and others. Compared to either the land use or landscape, the combination of them might be more useful in indicating PM_{10} concentration levels. And these results imply that more serious consideration of reasonable land use configurations could be a promising way to improve the air quality in urban sprawl, and China's "Two Oriented Society" policy is a sustainable urban development strategy for developing countries to effectively control urban air quality.

Author Contributions: This research was designed and written by Bin Zou, Shan Xu, Troy Sternberg and Xin Fang. All authors contributed to the analysis and conclusions, and revised the paper. All authors read and approved the final manuscript.

Conflicts of Interest: The authors declare no conflict of interest.

References

1. Pereira, P.; Monkevičius, A.; Siarova, H. Public perception of environmental, social and economic impacts of urban sprawl in Vilnius. *Soc. Stud.* **2014**, *6*, 259–290. [CrossRef]

2. Marquez, L.O.; Smith, N.C. A framework for linking urban form and air quality. *Environ. Model. Softw.* **1999**, *14*, 541–548. [CrossRef]

3. De Ridder, K.; Lefebre, F.; Adriaensen, S.; Arnold, U.; Beckroege, W.; Bronner, C.; Damsgaard, O.; Dostal, I.; Dufek, J.; Hirsch, J.; et al. Simulating the impact of urban sprawl on air quality and population exposure in the German Ruhr area. Part I: Reproducing the base state. *Atmos. Environ.* **2008**, *42*, 7059–7069. [CrossRef]

4. Stone, B., Jr. Urban sprawl and air quality in large US cities. *J. Environ. Manag.* **2008**, *86*, 688–698. [CrossRef] [PubMed]

5. Martins, H. Urban compaction or dispersion? An air quality modelling study. *Atmos. Environ.* **2012**, *54*, 60–72. [CrossRef]

6. Zou, B.; Peng, F.; Wan, N.; Mamady, K.; Wilson, G.J. Spatial cluster detection of air pollution exposure inequities across the United States. *PLoS ONE* **2014**, *9*, e91917. [CrossRef] [PubMed]

7. Zeng, C.; Liu, Y.; Stein, A.; Jiao, L. Characterization and spatial modeling of urban sprawl in the Wuhan Metropolitan Area, China. *Int. J. Appl. Earth Obs. Geoinformation* **2015**, *34*, 10–24. [CrossRef]

8. Clark, L.P.; Millet, D.B.; Marshall, J.D. Air quality and urban form in US urban areas: Evidence from regulatory monitors. *Environ. Sci. Technol.* **2011**, *45*, 7028–7035. [CrossRef] [PubMed]

9. Bandeira, J.M.; Coelho, M.C.; Sa, M.E.; Tavares, R.; Borrego, C. Impact of land use on urban mobility patterns, emissions and air quality in a Portuguese medium-sized city. *Sci. Total Environ.* **2011**, *409*, 1154–1163. [CrossRef] [PubMed]

10. Zou, B.; Wilson, J.G.; Zhan, F.B.; Zeng, Y. Air pollution exposure assessment methods utilized in epidemiological studies. *J. Environ. Monit.* **2009**, *11*, 475–490. [CrossRef] [PubMed]

11. Zou, B.; Wang, M.; Wan, N.; Wilson, J.G.; Fang, X.; Tang, Y. Spatial modeling of $PM_{2.5}$ concentrations with a multifactoral radial basis function neural network. *Environ. Sci. Pollut. Res.* **2015**, *22*, 10395–10404. [CrossRef] [PubMed]

12. Civerolo, K.; Hogrefe, C.; Lynn, B.; Rosenthal, J.; Ku, J.-Y.; Solecki, W.; Cox, J.; Small, C.; Rosenzweig, C.; Goldberg, R.; et al. Estimating the effects of increased urbanization on surface meteorology and ozone concentrations in the New York City metropolitan region. *Atmos. Environ.* **2007**, *41*, 1803–1818. [CrossRef]

13. De Ridder, K.; Lefebre, F.; Adriaensen, S.; Arnold, U.; Beckroege, W.; Bronner, C.; Damsgaard, O.; Dostal, I.; Dufek, J.; Hirsch, J.; et al. Simulating the impact of urban sprawl on air quality and population exposure in the German Ruhr area. Part II: Development and evaluation of an urban growth scenario. *Atmos. Environ.* **2008**, *42*, 7070–7077. [CrossRef]

14. Kahyaoğlu-Koračin, J.; Bassett, S.D.; Mouat, D.A.; Gertler, A.W. Application of a scenario-based modeling system to evaluate the air quality impacts of future growth. *Atmos. Environ.* **2009**, *43*, 1021–1028. [CrossRef]

15. Zou, B.; Luo, Y.; Wan, N.; Zheng, Z.; Sternberg, T.; Liao, Y. Performance comparison of LUR and OK in $PM_{2.5}$ concentration mapping: A multidimensional perspective. *Sci. Rep.* **2015**, *5*, 8698. [CrossRef] [PubMed]

16. Weng, Q.; Yang, S. Urban air pollution patterns, land use, and thermal landscape: An examination of the linkage using GIS. *Environ. Monit. Assess.* **2006**, *117*, 463–489. [CrossRef] [PubMed]

17. Bereitschaft, B.; Debbage, K. Urban form, air pollution, and CO_2 emissions in large U.S. metropolitan areas. *Prof. Geogr.* **2013**, *65*, 612–635. [CrossRef]

18. Weber, N.; Haase, D.; Franck, U. Assessing modelled outdoor traffic-induced noise and air pollution around urban structures using the concept of landscape metrics. *Landsc. Urban. Plan.* **2014**, *125*, 105–116. [CrossRef]

19. McCarty, J.; Kaza, N. Urban form and air quality in the United States. *Landsc. Urban Plan.* **2015**, *139*, 168–179. [CrossRef]

20. Zou, B.; Pu, Q.; Muhammad, B.; Weng, Q.; Zhai, L.; Nichol, J. High-resolution satellite mapping of fine particulates based on geographically weighted regression. *IEEE Geosci. Remote Sens. Lett.* **2016**, *13*, 495–499. [CrossRef]

21. Chen, L.; Bai, Z.; Kong, S.; Han, B.; You, Y.; Ding, X.; Du, S.; Liu, A. A land use regression for predicting NO_2 and PM_{10} concentrations in different seasons in Tianjin region, China. *J. Environ. Sci.* **2010**, *22*, 1364–1373. [CrossRef]

22. Kloog, I.; Koutrakis, P.; Coull, B.A.; Lee, H.J.; Schwartz, J. Assessing temporally and spatially resolved $PM_{2.5}$ exposures for epidemiological studies using satellite aerosol optical depth measurements. *Atmos. Environ.* **2011**, *45*, 6267–6275. [CrossRef]

23. Vienneau, D.; de Hoogh, K.; Bechle, M.J.; Beelen, R.; van Donkelaar, A.; Martin, R.V.; Millet, D.B.; Hoek, G.; Marshall, J.D. Western European land use regression incorporating satellite- and ground-based measurements of NO_2 and PM_{10}. *Environ. Sci. Technol.* **2013**, *47*, 13555–13564. [CrossRef] [PubMed]

24. Hoek, G.; Beelen, R.; de Hoogh, K.; Vienneau, D.; Gulliver, J.; Fischer, P.; Briggs, D. A review of land-use regression models to assess spatial variation of outdoor air pollution. *Atmos. Environ.* **2008**, *42*, 7561–7578. [CrossRef]

25. Moore, D.K.; Jerrett, M.; Mack, W.J.; Kunzli, N. A land use regression model for predicting ambient fine particulate matter across Los Angeles, CA. *J. Environ. Monit.* **2007**, *9*, 246–252. [CrossRef] [PubMed]

26. Kloog, I.; Nordio, F.; Coull, B.A.; Schwartz, J. Incorporating local land use regression and satellite aerosol optical depth in a hybrid model of spatiotemporal $PM_{2.5}$ exposures in the Mid-Atlantic states. *Environ. Sci. Technol.* **2012**, *46*, 11913–11921. [CrossRef] [PubMed]

27. Marcon, A.; de Hoogh, K.; Gulliver, J.; Beelen, R.; Hansell, A.L. Development and transferability of a nitrogen dioxide land use regression model within the Veneto region of Italy. *Atmos. Environ.* **2015**, *122*, 696–704. [CrossRef]

28. Baldasano, J.; Valera, E.; Jimenez, P. Air quality data from large cities. *Sci. Total Environ.* **2003**, *307*, 141–165. [CrossRef]

29. Chan, C.K.; Yao, X. Air pollution in mega cities in China. *Atmos. Environ.* **2008**, *42*, 1–42. [CrossRef]

30. Rohde, R.A.; Muller, R.A. Air pollution in China: Mapping of concentrations and sources. *PLoS ONE* **2015**, *10*, e0135749.

31. USGS Global Visualization Viewer (USGS). Available online: http://glovis.usgs.gov/ (accessed on 12 August 2014).

32. ENVI: The Environment for Visualizing Images. Available online: https://www.harrisgeospatial.com/docs/using_envi_home.html (accessed on 15 July 2015).

33. FRAGSTATS: Spatial Pattern Analysis Program for Quantifying Landscape Structure. Portland (OR): USDA Forest Service, Pacific Northwest Research Station. Available online: http://www.fs.fed.us/pnw/pubs/pnw_gtr351.pdf (accessed on 15 July 2015).

34. Gustafson, E.J. Quantifying landscape spatial pattern: What is the state of the art? *Ecosystems* **1998**, *1*, 143–156. [CrossRef]

35. Lv, Z.-Q.; Dai, F.-Q.; Sun, C. Evaluation of urban sprawl and urban landscape pattern in a rapidly developing region. *Environ. Monit. Assess.* **2011**, *184*, 6437–6448. [CrossRef] [PubMed]

36. Ji, W.; Ma, J.; Twibell, R.W.; Underhill, K. Characterizing urban sprawl using multi-stage remote sensing images and landscape metrics. *Comput. Environ. Urban. Syst.* **2006**, *30*, 861–879. [CrossRef]

37. FRAGSTATS. Available online: http://www.umass.edu/landeco/research/fragstats/downloads/fragstats_downloads.html (accessed on 12 October 2013).

38. China Environmental Monitoring Center. Available online: http://113.108.142.147:20035/emcpublish/ (accessed on 1 January 2014).

39. Level 1 and Atmosphere Archive and Distribution System (LAADS). Available online: https://earthdata.nasa.gov/about/daacs/daac-laads (accessed on 20 May 2014).

40. Statistical Bureau of Hunan Province. Available online: http://www.hntj.gov.cn/ (accessed on 21 May 2014).

41. Hunan Meteorology. Available online: http://www.hnqx.gov.cn/ (accessed on 22 May 2014).

42. SPSS: IBM SPSS Software. Available online: http://www.ibm.com/analytics/us/en/technology/spss/spss-trials.html (accessed on 25 June 2015).

43. Hunan Statistical Year Book 2013. Available online: http://www.chinabookshop.net/hunan-statistical-yearbook-2013-p-18748.html (accessed on 4 January 2015).

44. Liu, H.-L.; Shen, Y.-S. The impact of green space changes on air pollution and microclimates: A case study of the Taipei metropolitan area. *Sustainability* **2014**, *6*, 8827–8855. [CrossRef]

45. Bright, V.B.; Bloss, W.J.; Cai, X. Urban street canyons: Coupling dynamics, chemistry and within-canyon chemical processing of emissions. *Atmos. Environ.* **2013**, *68*, 127–142. [CrossRef]